ADP-ribosylation factor (ARF)-like 7 (ARL7) is induced by cholesterol loading and participates in apolipoprotein AI-dependent cholesterol export

Thomas Engel[a,*], Aloys Lueken[a], Günther Bode[a,b], Uwe Hobohm[c], Stefan Lorkowski[a], Bernhard Schlueter[b], Stephan Rust[a], Paul Cullen[a], Michael Pech[c], Gerd Assmann[a,b], Udo Seedorf[a]

[a]*Institut für Arteriosklerosеforschung, Westfälische Wilhelms-Universität, Domagkstr. 3, D-48149 Münster, Germany*
[b]*Institut für Klinische Chemie und Laboratoriumsmedizin, Westfälische Wilhelms-Universität, Domagkstr. 3, D-48149 Münster, Germany*
[c]*Preclinical Research, F. Hoffmann La-Roche AG, CH-4060 Basel, Switzerland*

Received 12 February 2004; revised 7 April 2004; accepted 8 April 2004

Available online 3 May 2004

Edited by Felix Wieland

Abstract Here, we identify ADP-ribosylation factor (ARF)-like 7 (ARL7) as the only ARF- and ARL-family member whose mRNA-expression is induced by liver X-receptor/retinoid X-receptor agonists or cholesterol loading in human macrophages. Moreover, subcellular distribution of mutant and wild type ARL7-enhanced green fluorescent protein (EGFP) supports that ARL7 may be involved in a vesicular transport step between a perinuclear compartment and the plasma membrane. Therefore, we investigated the effect of ARL7 over-expression on the cholesterol secretory pathway. We found that expression of wild type and dominant active ARL7-EGFP stimulated the rate of apolipoprotein AI-specific cholesterol efflux 1.7- and 2.8-fold. In contrast, expression of the dominant negative form of ARL7-EGFP led to ~50% inhibition of cholesterol efflux. This data is consistent with a model in which ARL7 is involved in transport between a perinuclear compartment and the plasma membrane apparently linked to the ABCA1-mediated cholesterol secretion pathway.

Keywords: ADP-ribosylation factor; Ras-related; ADP-ribosylation factor-like 7; GTPase; Cholesterol; Transport

1. Introduction

Cellular lipid content and distribution is tightly controlled at the stages of lipoprotein uptake, lipid synthesis, sorting, storage, and export [1]. ATP-binding cassette transporter ABCA1 controls removal of excess cholesterol by high density lipoproteins (HDL), the initial step of "reverse cholesterol transport" (RCT) [2–4]. The RCT pathway is essential for virtually all cells but especially for the macrophage which is subject to high non-regulated intake of cholesterol and other lipids due to uptake and degradation of dead and apoptotic cells as well as modified lipoproteins. The transformation of macrophages to foam cells is thought to initiate atherosclerotic plaque formation in the arterial wall which may end in coronary heart disease and stroke, the most prominent causes of death in the western world [5].

ApoAI and HDL are extracellular acceptors for excess cholesterol. Tangier disease, a rare autosomal disease caused by mutations in ABCA1, is characterized by complete lack of HDL and massive foam-cell formation, primarily in the reticulo-endothelial system, due to defective lipid export capacity of the macrophage [6–8]. The precise molecular mechanism of HDL-formation by ABCA1 needs further clarification. Since vesicular transport mediates some part of cellular cholesterol transport, it may be assumed that cholesterol trafficking to the plasma membrane depends on target-specific vesicular transport systems which mediate cholesterol flux from intracellular pools to ABCA1 located at the plasma membrane and recycling endosomes. ADP-ribosylation factors (ARFs) represent Ras-related small regulatory GTPases which control vesicular transport in the secretory and endosomal pathway at the stage of vesicle budding [9]. In addition, members of this family regulate various cellular functions such as cytoskeleton formation/remodelling or the activity of phospholipase D [10–12]. ARF-like proteins (ARLs) are thought to have a similar function [13]. The aim of the present study was to identify ARLs or ARFs which may be involved in cholesterol transport upon ABCA1-meditated cholesterol secretion. Our results indicate that, among a great variety of ARFs and ARLs, ARL7, which was cloned initially as a GTPase with rapid nucleotide exchange and a putative nuclear function [14], is the only family member whose expression is induced significantly by liver X-receptor (LXR) and retinoid X-receptor (RXR) agonists (T0901317 and RO-26-4456) or cholesterol-loading. Since this regulation implied that ARL7 may be involved in RCT, we studied its intracellular trafficking and the effect of several ARL7 mutants on apoAI-dependent cholesterol efflux. The results of these studies supported an involvement of ARL7 in RCT. We currently presume that ARL7 contributes to a vesicular transport step between a perinuclear compartment and an ABCA1 accessible cholesterol pool at the plasma membrane.

* Corresponding author. Fax: +49-251-83-56205.
E-mail address: engeltho@uni-muenster.de (T. Engel).

Abbreviations: ABC, ATP binding cassette; acLDL, acetylated low density lipoprotein; apo, apolipoprotein; ATP, adenosine triphosphate; EGFP, enhanced green fluorescent protein; HDL, high density lipoprotein; LDL, low density lipoprotein; PCR, polymerase chain reaction; RCT, reverse cholesterol transport; wt, wild type

0014-5793/$22.00
doi:10.1016/j.febslet.2004.04.048

2. Materials and methods

2.1. Reagents and cells

LXR and RXR agonist T0901317 and RO-26-4456, respectively, were kindly provided by F. Hoffmann La-Roche, Basel, and used at a concentration of 0.1 and 1 μM, respectively. Anti-ARF6 monoclonal antibody (clone 3A1) was purchased from Santa Cruz Biotechnology. Acetylated low density lipoprotein (acLDL) was prepared and human monocytes were obtained and maintained as previously described [15]. HeLa cells (DSMZ) were maintained in DMEM/10% FCS/penicillin (100 units/ml)/streptomycin (0.1 mg/ml) in a humidified incubator at 37 °C and 5% CO_2.

2.2. Quantitative real-time PCR assay

Assays were performed as previously described [15] using a GeneAmp 7900HT sequence detection system (ABI). The following as well as established [15] primer pairs were used for amplification: ARF1, 5′-CAGACTGCGATCAATTCTGC-3′, 5′-GACAAGCACATGGCTATGGA-3′; ARF2, 5′-AATAACACCTTCGCTGTCTGG-3′, 5′-AAGTGAGCCTTGATGTG TGC-3′; ARF3, 5′-TGCAAACAAACAGGATCTGC-3′, 5′-ACCAGTTACGGTGACGAAGG-3′; ARF4, 5′-GACTCCTGGCCTACATCAGC-3′, 5′-CAATTCTTTGCAACCAGCAC-3′; ARF5, 5′-AGAAGCAGATGCGGATTCTC-3′, 5′-TATGGTTGGGATGGTGGTG-3′; ARF6, 5′-TTGTTGGCT TTGCGTTAGG-3′, 5′-TTCCCATTCTGCTGGAAGTC-3′; ARL1, 5′-CACTTGGGTTACCTGCCTTG-3′, 5′-AACCATTCCATTGCCTCATC-3′; ARL2, 5′-GGCTCCTGACCATT CTGAAG-3′, 5′-TCAGGATGGTTGTCTTTCCAG-3′; ARL3, 5′-GACATCAGCCACATCACACC-3′, 5′-TCCTCTGTCCA CCAATGTCC-3′; ARL4, 5′-TAGCAATGGGTGAACTGAGC-3′, 5′-CCTTCCTTTAGGCCATCTCC-3′; ARL5, 5′-GCC AAGGACTTGAATGGATG-3′, 5′-GCAGCTTTCAGGTAAAGTCCAG-3′; ARL6, 5′-AGAAGGCTTGCAAGAAGGTG-3′, 5′-TTGAAAATTGCTGAGGTTTCC-3′; ARL7, 5′-ATGGATGGATGAGCGAGAAC-3′, 5′-CATTTGGGTGCAGAGATTCC-3′.

2.3. 3′-RACE

Total RNA was isolated as described [15]. 3′-RACE was performed using the 3′-RACE system according to the manufacturers guidelines (Invitrogen) with a gene-specific primer 5′-CTTCAACACCGAGAAGATCAAGCTG-3′ in the coding sequence of the open reading frame of the ARL7 cDNA. Polymerase chain reaction (PCR) products obtained were purified on columns (Qiagen) and sequenced directly using the ABI PRISM® BigDye™ Terminators v2.0 Cycle Sequencing Kit (ABI). Sequencing reactions were separated on an ABI-PRISM 3700 DNA Analyzer (ABI).

2.4. Expression of ARL7 in HeLa cells

Coding sequence of ARL7 with Kozak consensus sequence and lacking a stop codon was amplified from human macrophage cDNA with flanking *Bam*HI and *Hin*dIII restriction sites and inserted in frame with enhanced green fluorescent protein (EGFP) into pEGFP-N1 vector (Clontech). Point mutations were introduced using QuikChange Kit according to the manufacturers guidelines (Stratagene). All amplified sequences were verified by DNA sequencing, as described above. For transient expression experiments 1.6×10^6 trypsinized HeLa cells in 0.4 ml DMEM were transfected with 10 μg plasmid DNA using an electroporator equipped with a capacitance extender (GenePulser II, BioRad) at 975 μF and 230 V. Cells were seeded on six 12 mm diameter cover slips in 24-well dishes and fixed with 4% PFA in PBS 12–48 h post-transfection. Cover slips were mounted on cover slides using Mowiol and viewed with a Zeiss Axioskop equipped with a CCD camera and fluorescein filter set. Images were processed using Adobe Photoshop 7.0. Stable transfections were performed as above with 4×10^6 cells in 0.4 ml DMEM. Cells were seeded in ten tissue culture dishes with 15 cm diameter. For selection 0.5 mg/ml G418 (Gibco) was added to complete medium. Medium was changed every 3–4 days. Single clones were selected after 3 weeks using cloning cylinders (Bellco Glass), and screened by fluorescence microscopy and Western-blot analysis using our polyclonal ARL7 antibody.

2.5. Polyclonal ARL7 antibody

Synthetic peptides corresponding to aa 144–159 and 168–182 of human ARL7, respectively, containing a cysteine at the amino-terminal position were synthesized and coupled to keyhole limpet hemocyanine. Rabbits were immunized with a mixture of both immunogens using the DoubleX-Service (Eurogentec). Specific IgGs were purified from the antiserum according to established procedures [16] using a matrix consisting of antigen coupled to Sulfolink-beads (Pierce). Antibodies were biotinylated using the Biotin Labeling Kit (Roche Diagnostics).

2.6. Immune-precipitations

Ten million cells were washed with PBS and scraped off the plate in ice cold lysis buffer (0.3 M NaCl/0.1 M Tris/HCl, pH 7.4/2% Triton X-100/1% sodium deoxycholate) supplemented with Complete protease inhibitor cocktail (Roche). Cells were lysed for 1 h on ice in lysis buffer. Subsequent steps were performed at 4 °C on a rotating wheel. Supernatants were obtained (30 min $30\,000 \times g$, JA20, Beckman), an equal volume of water was added and supernatants were precleared for 1 h using protein G-Sepharose4B beads (Amersham). Antigen was immune-precipitated by incubating the supernatants with IgGs prebound to protein G-Sepharose4B beads for 2 h. Beads were harvested and washed according to the manufacturers guidelines (Immune-precipitation Kit, Roche) and processed for Western-blot analysis.

2.7. Western-blot analysis

Samples were lysed in Laemmli sample buffer supplemented with ß-mercaptoethanol and separated on 12.5% SDS–PAGE gels [17]. Protein was transferred onto Protran nitrocellulose filters (Schleicher & Schuell). For detection with HRP-labeled secondary antibody 5% dry skim milk in PBS/0.1% Tween 20 was used for blocking the filter and for antibody incubations, for detection of biotinylated antibody 2.5% BSA in PBS/0.1% Tween 20 was used instead. For detection horseradish peroxidase-labeled secondary antibody (BioRad) or horseradish peroxidase-streptavidin, respectively, ECL system and Hyperfilm ECL was used (Amersham). Developed films were scanned and quantified using ImageJ software (http://rsb.info.nih.gov/ij/).

2.8. Cholesterol efflux measurement

Cells were grown in a 24-well tissue culture plate. Confluent cells were labeled overnight with 0.5 ml/well of DMEM/0.2% BSA/1 μM T0901317/100 nM RO-26-4456 containing 2 μCi [^{3}H]-cholesterol (NEN-DuPont) per well. Cells were washed on ice with cold DMEM/0.5% BSA and DMEM twice for 5 min each. 0.3 ml efflux medium consisting of DMEM/0.2% BSA/1 μM T0901317/100 nM RO-26-4456 with or without 10 μg apolipoprotein AI was added for 4 h. Medium was harvested, cells were removed by centrifugation and radioactivity of an 0.25 ml aliquot was determined. Cells were lysed by adding 0.25 ml 0.1 M NaOH/0.15 M NaCl. After 10 min lysates and centrifuged cells were collected in scintillation vials, plates were washed again with 0.25 ml 0.1 M NaOH/0.15 M NaCl and radioactivity of the samples was determined. The fractional apoAI specific cholesterol efflux was determined and normalized to the value obtained for HeLa cells.

3. Results

3.1. Differential expression analysis

As candidates for differential expression analysis we chose members of the ARF and ARF-like family, which may be involved in vesicular transport steps within the cell requiring coat protein assembly [9]. The study was performed using reverse transcription quantitative real-time PCR at different cholesterol loading states of the macrophage. acLDL was used for cholesterol-loading, 2-hydroxypropyl-β-cyclodextrin for cholesterol-depletion. As shown in Fig. 1, ARL7 was the only studied family member which showed a direct and strong response to cholesterol loading. The expression level of ARL7 mRNA was induced further by applying synthetic agonists specific for the nuclear receptors LXR and RXR and was repressed by cellular sterol unloading with 2-hydroxypropyl-β-cyclodextrin. Such an expression pattern is similar to that observed for the cellular lipid exporters ATP-binding cassette transporter family members ABCA1 and ABCG1 [15,18]. The

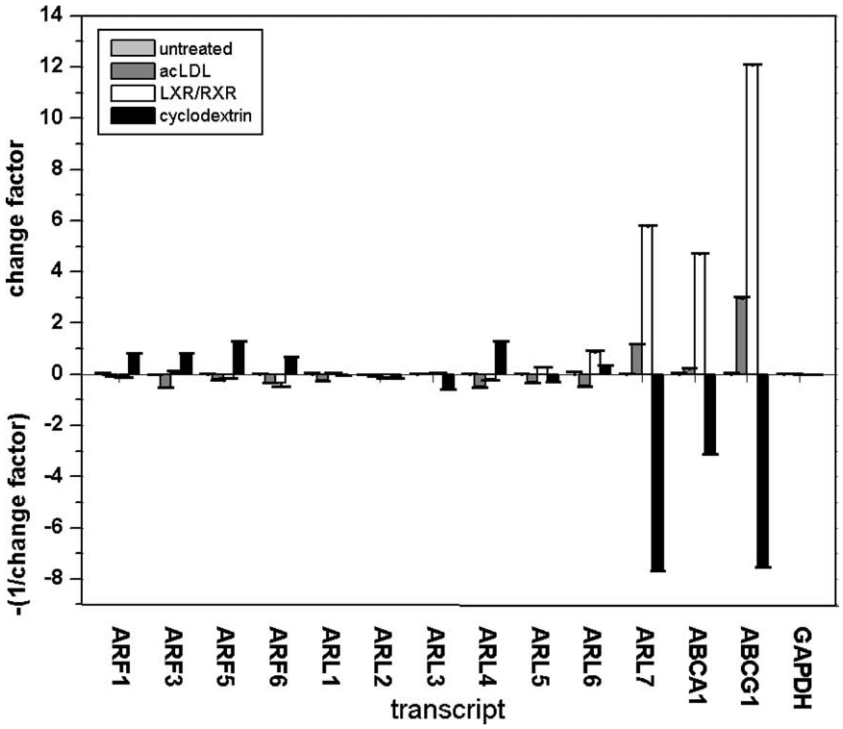

Fig. 1. ARL7 gene expression is sterol sensitive. Human monocyte-derived macrophages were incubated for 24 h without added substance (light grey), and in the presence of 80 μg acetylated LDL/ml (grey), synthetic LXR and RXR agonists (white) or 2% 2-hydroxypropyl-β-cyclodextrin (black), respectively. Quantitative real-time PCR analysis was performed, as described in Section 2. Expression changes for transcripts of ARL7 as well as for its family members ARL1–6, ARF1, -3, -5, -6, and ABC transporters ABCA1 and ABCG1 as well as glyceraldehyde-3-phosphate-dehydrogenase (GAPDH) as a housekeeping gene are shown. Samples were measured as triplicates and standard errors are given as error bars.

range of expression observed for the ARL7 transcript was a difference of 5.87 ± 0.12 cycles at threshold corresponding to a 58.5-fold ($\pm$1.1-fold) expression difference. Most of the other ARF-family members showed almost no or the opposite regulation, especially during cholesterol removal.

High density DNA array analysis with Hu35KsubA-D and HuGeneFl chip set (Affymetrix) that was performed to obtain a comprehensive set of data on cholesterol-dependent gene regulation in human macrophages (Hobohm and Pech, unpublished) confirmed the real-time quantitative PCR results. Features on the chip surface corresponding to GenBank Expressed Sequence Tag (EST)-clone AA213410, presumably corresponding to the 3′-end of the human ARL7 cDNA, displayed the same expression behavior. 3′-Rapid amplification of cDNA end (3′-RACE) analysis confirmed that EST-clone AA213410 is part of the ARL7 cDNA. The corresponding sequence was deposited as Acc. AJ579851 in the EMBL nucleotide database. Reverse transcription quantitative real-time PCR using primer pairs specific for amplification of AA213410 confirmed 3′-RACE results as identical cycles at threshold values and expression differences were observed for target regions in the coding sequence and the 3′-end of the ARL7-cDNA (not shown).

In order to test whether expression changes at the mRNA-level propagate to the protein level, we performed immune-precipitations using extracts from HeLa cells incubated with or without either LDL or synthetic LXR/RXR agonists, respectively. Enrichment of ARL7 by immune-precipitation was required since our ARL7 antibody was not sensitive enough to detect the endogenous ARL7 protein. As shown in Fig. 2, ARL7 protein was detected at the expected molecular weight of 24 kDa. Incubation of HeLa cells with LDL increased ARL7 protein content 1.8-fold and application of LXR/RXR agonist induced it further (3.2-fold compared to untreated cells), consistent with the changes of ARL7-mRNA. As a control, ARF6 protein content was not influenced by incubation with LDL or LXR/RXR agonist.

3.2. Expression studies

For functional characterization of ARL7 we generated a set of vectors allowing expression of ARL7-EGFP fusion proteins containing the wild type (wt) or mutant ARL7 sequences. ARL7(G2A) lacks a myristoylation site, ARL(T27N) represents the inactive GDP-bound (dominant negative) and ARL7(Q71L) the active GTP-bound state (dominant active). As shown in Fig. 3, wt and mutant ARL7-EGFP fusion proteins were transiently expressed in HeLa cells to the same extent. Our anti-ARL7 antibody detected the fusion proteins at the expected molecular weight of $\sim$50 kDa in all cases.

When detecting GFP epifluorescence of ARL7-EGFP expressing cells, a characteristic phenotype was the change in HeLa cell morphology: When wt ARL7-EGFP was expressed, green staining was detected within the cells and many intensely stained filopodia formed at the periphery of the cell, indicating interaction of ARL7 with components of the cytoskeleton (Fig. 4A). Filopodia and their intense labeling disappeared when cytochalasin D was added to the cells, whereas nocodazole had no effect (not shown). Thus, ARL7 is presumably involved in actin filament assembly and/or reorganization.

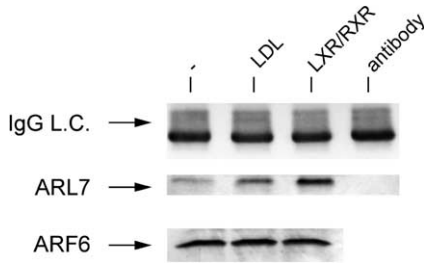

Fig. 2. ARL7 protein expression parallels mRNA expression. HeLa-cells were grown in complete medium without, with LDL or with synthetic LXR and RXR agonists for 24 h. Cells were harvested and processed for immune-precipitation analysis. Western blots were performed with a biotinylated rabbit anti-ARL7 antibody followed by streptavidin-horseradish peroxidase. ARL7 protein is detected at 24 kDa. As loading control IgG light chain of the anti-ARL7 antibody was detected using anti-rabbit IgG-horseradish peroxidase. ARF6 was detected in an aliquot of the cells used for the immune-precipitation and is not differentially expressed.

Unlike wt ARL7, the G2A mutant displayed a uniform cytoplasmic localization, most likely since it lacked its membrane attachment site (Fig. 4B). This mutation also inactivated the protein with respect to its effect on the cytoskeleton. The T27N mutant was present mainly on small punctate structures in the perinuclear region of the cell and did not lead to filopodia formation (Fig. 4C). Conversely, the Q71L mutant resulted in a very similar staining pattern and affected the cellular morphology the same way as wt ARL7 with less filopodia (Fig. 4D).

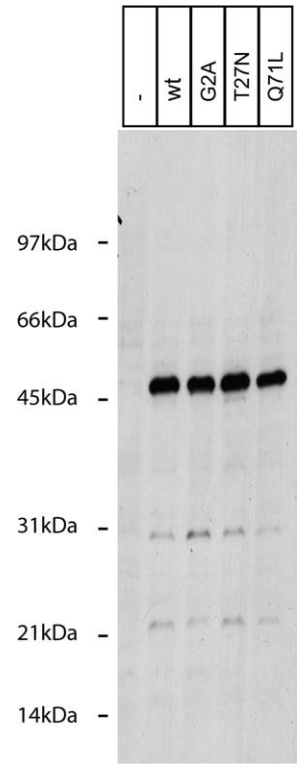

Fig. 3. Expression of ARL7-EGFP fusion proteins. HeLa-cells were transiently transfected with constructs coding for EGFP alone or for ARL7-EGFP-fusion proteins for 24 h. Western blots were performed with a rabbit anti-ARL7 antibody and goat anti-rabbit horseradish peroxidase. ARL7-EGFP-fusion protein is detected at ~50 kDa.

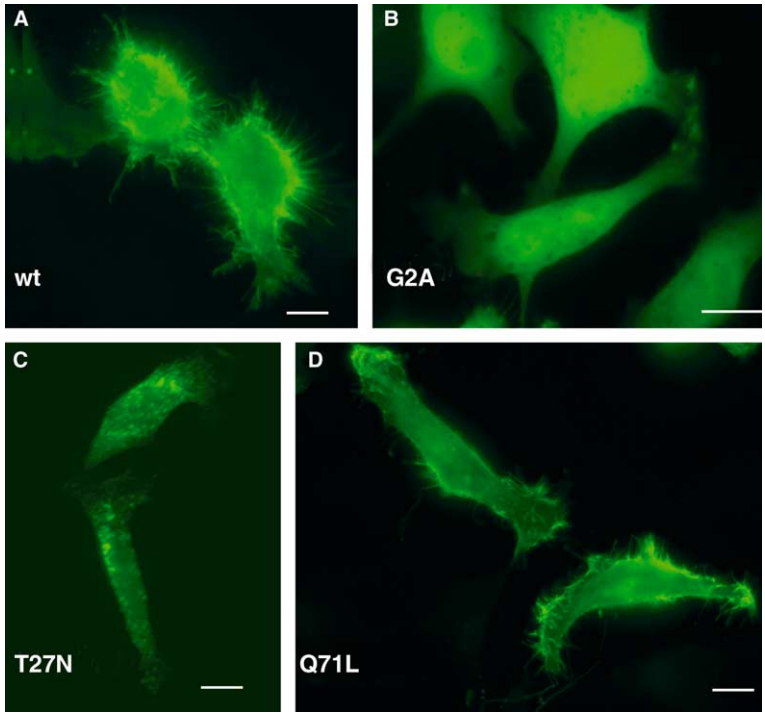

Fig. 4. Subcellular distribution of wt and mutant ARL7-EGFP fusion proteins Human ARL7 fused to EGFP was transiently expressed in HeLa cells for 24 h. (A) ARL7(wt), (B) ARL7(G2A), (C) ARL7(T27N), (D) ARL7(Q71L). Cells were fixed and epifluorescence was recorded. Scale bars represent 10 μm.

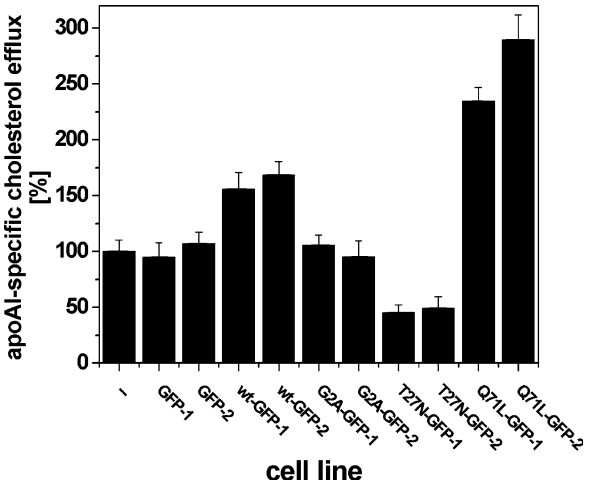

Fig. 5. Effect of ARL7 on cellular cholesterol efflux. HeLa cells either untransfected or stably expressing wt and mutant ARL7-EGFP fusion proteins or EGFP were used for cholesterol efflux measurements as described in Materials and Methods. Triplicate measurements were performed.

3.3. Cholesterol efflux measurements

Given this intracellular localization pattern, we next studied whether ARL7 may play a role in cellular cholesterol export. For these studies, we generated a series of HeLa cell lines stably expressing the above mentioned ARL7-EGFP fusion proteins. These lines were labeled with [^{3}H]-cholesterol and incubated in the presence or absence of apoAI with efflux medium containing BSA, 1 μM of T0901317 and 0.1 μM of RO-26-4456. Subsequently, radioactivity was determined in the medium and cell lysates and the fractional apoAI specific cholesterol efflux was evaluated as described in Section 2. As shown in Fig. 5, expression of wt ARL7-EGFP led to a moderate stimulation of the fractional apoAI specific cholesterol efflux (~1.7-fold, $p < 0.05$). Expression of dominant-active ARL7 resulted in more pronounced stimulatory effect (almost 3-fold stimulation, $p < 0.001$). In contrast, the dominant negative form inhibited the fractional apoAI specific cholesterol efflux by ~50% ($p < 0.001$). Moreover, EGFP as well as ARL7(G2A)-EGFP used as controls had no effect.

4. Discussion

The results of this study support that an ARF-like protein, ARL7, may play a role in cellular cholesterol secretion. According to this concept, ARL7 would participate in the pathway which enables the cell to export cholesterol when the cellular level of cholesterol is rising and cholesterol secretion is necessary in order to protect the cell from the devastating effects resulting from cholesterol overloading. We could demonstrate that ARL7 expression is regulated in a coordinate manner with other components of the cholesterol secretion machinery, especially ABCA1. It is conceivable that efficient cholesterol export depends on efficient transport of cholesterol from intracellular pools to the plasma membrane where it is desorbed either non-specifically into the extracellular space or transferred in a specific manner onto apolipoproteins or nascent lipoprotein particles via the ABCA1-pathway [1,19–21]. Hence, simultaneous upregulation of ABCA1 and ARL7 may provide a useful mechanism to increase the capacity of the cell to transfer excess cholesterol to an ABCA1-accessible cholesterol pool at or close to the plasma membrane.

Since dominant active and wt ARL7 strongly stain filopodia the assumption that ARL7 is involved in trafficking towards the plasma membrane is supported by our results in analogy to similar data on ARF6 [22–24]. Dominant negative ARL7 resides on perinuclear structures which lets us assume that these structures are the starting point of ARL7-mediated transport vesicle formation, similarly as was proposed for dominant negative ARF6 [23].

Since we could demonstrate that ARL7-mediated stimulation of cholesterol secretion depended on the presence of apoAI it seems likely that ARL7 acts in concert with ABCA1. According to previous studies, ABCA1 is transported on a retroendocytic route in a variety of cell types [25,26]. In addition, uptake and resecretion of apolipoproteins that interact with ABCA1 has been reported [20,27–29]. Thus, it is possible that some of the effects of ARL7 on apoAI-dependent cholesterol efflux are in fact secondary to modulation of ABCA1 transport or other means, such as altered half life of ABCA1 or modulation of apoAI and/or ABCA1 endocytic transport. Clearly, further studies will be required in order to evaluate these possibilities.

Moreover, some caution must remain with respect to the interpretation of our data. Over-expression of the two ARL7 forms (ARL7-EGFP and ARL7(Q71L)-EGFP) which stimulated cholesterol efflux were associated with quite extensive alterations of cell morphology. Most striking was the formation of filopodia, implying that ARL7 over-expression altered cytoskeleton assembly and/or remodeling. We presume that some of these changes may have been due to accumulation of ARL7-EGFP and ARL7(Q71L)-EGFP at the terminus of their transport route, presumably as a consequence of a very slow return to their starting point. The latter effect may have been caused by a limited supply of ARL7-specific effectors (e.g. GTPase activating protein, GAP), or changes in the kinetics of intracellular transport routes resulting from over-expression in a similar manner as was proposed in the case of ARFs by D'Souza-Schorey [23]. One very obvious consequence resulting from filopodia formation was a considerable increase of the cell surface area. This may have increased the efficiency by which apoAI extracted cholesterol from cholesterol-rich microdomains at the level of the plasma membrane essentially in an artifactual manner. However, our observation that the quite significant inhibition of cholesterol efflux which resulted from expression of the dominant negative form of ARL7 occurred in the absence of any detectable changes of cell morphology supports the specificity of the ARL7-mediated effect very strongly. Thus, we think that it is justified to conclude that ARL7 contributes to apoAI-dependent cholesterol secretion in a specific manner.

The present results on intracellular localization and trafficking of ARL7 differ from a previous study which led to the assumption that ARL7 may be located in the nucleus [14]. This assumption based on the use of a synthetic construct consisting of GFP fused to the last 20 amino acids of the ARL7 carboxy-terminus. This peptide exhibits similarity to nuclear localization signals because it contains nine arginine or lysine residues. In contrast to the previous study, we used the full length ARL7 sequence fused at the carboxy-terminus to EGFP. None of the various ARL7-EGFP fusion constructs that were used in our study were able to direct a significant fraction of the fusion

proteins into the nucleus. Conversely, it could be demonstrated by immunocytochemistry that a fraction of ARL4, which is a close relative of ARL7, is in fact located in the nucleus of cultured Sertoli and neuroblastoma cells [14,30]. Thus, it cannot be excluded at present that the EGFP fusion at the carboxy-terminus of ARL7 that was used in our study inhibited its import into the nucleus. Nevertheless, in the case of ARL4, a significant fraction of the protein could be found associated with the cytoplasmic vesicle fraction in addition to its nuclear localization. According to our data the situation appears to be similar for ARL7, because we could demonstrate that a significant fraction of the ARL7 protein is targeted to a cytoplasmic vesicle fraction destined to be transported to the plasma membrane.

Currently, it is not entirely clear how various mammalian ARLs are targeted to their correct destinations in the cell. However, it was shown recently for two yeast ARLs, Arl1p and Arl3p, that Golgi localization of Arl1p is regulated via a cascade in which the GTPase cycle of Arl3p regulates Golgi localization of Arl1p [31]. Thus, it is conceivable that the GTPase cycle domain may be an essential structural requirement for ARL targeting in a physiological context. Moreover, it is evident from our results obtained with the myristoylation-defective mutant ARL7(G2A)-EGFP that ARL7 myristoylation is essential for its recruitment to cytoplasmic vesicles. Thus, we think that our strategy to use EGFP fusions with the full length ARL7 sequence provides a good indication for ARL7 targeting and trafficking under in vivo conditions.

Acknowledgements: We are glad to thank the following persons for their excellent technical assistance: Renate Berfeld, Walburga Hanekamp, Hildegard Hünting, Gaby Inkmann, and Karin Tegelkamp. This work forms part of the doctoral thesis of A.L. We are grateful to Dr. Manfred Fobker and Dr. Roch Nofer for critical reading of the manuscript. We thank F. Hoffmann La-Roche, Basel, Switzerland for financial support.

References

[1] Maxfield, F.R. and Wustner, D. (2002) J. Clin. Invest. 110, 891–898.
[2] Glomset, J.A. (1968) J. Lipid Res. 9, 155–167.
[3] Fielding, C.J. and Fielding, P.E. (1997) J. Lipid Res. 38, 1503–1521.
[4] Brewer Jr., H.B. and Santamarina-Fojo, S. (2003) Am. J. Cardiol. 91, 3E–11E.
[5] Ross, R. (1999) N. Engl. J. Med. 340, 115–126.
[6] Rust, S. et al. (1999) Nat. Genet. 22, 352–355.
[7] Bodzioch, M. et al. (1999) Nat. Genet. 22, 347–351.
[8] Marcil, M. et al. (1999) Lancet 354, 1341–1346.
[9] Rothman, J.E. and Wieland, F.T. (1996) Science 272, 227–234.
[10] Stamnes, M. (2002) Curr. Opin. Cell Biol. 14, 428–433.
[11] Moss, J. and Vaughan, M. (1999) Mol. Cell Biochem. 193, 153–157.
[12] Exton, J.H. (2002) FEBS Lett. 531, 58–61.
[13] Lu, L., Horstmann, H., Ng, C. and Hong, W. (2001) J. Cell Sci. 114, 4543–4555.
[14] Jacobs, S., Schilf, C., Fliegert, F., Koling, S., Weber, Y., Schurmann, A. and Joost, H.G. (1999) FEBS Lett. 456, 384–388.
[15] Engel, T., Lorkowski, S., Lueken, A., Rust, S., Schluter, B., Berger, G., Cullen, P. and Assmann, G. (2001) Biochem. Biophys. Res. Commun. 288, 483–488.
[16] Harlow, E. and Lane, D. (1988) Cold Spring Harbor Laboratory. Cold Spring Harbor, New York.
[17] Laemmli, U.K. (1970) Nature 227, 680–685.
[18] Repa, J.J. et al. (2000) Science 289, 1524–1529.
[19] Liscum, L. and Munn, N.J. (1999) Biochim. Biophys. Acta 1438, 19–37.
[20] Oram, J.F. (2002) Curr. Opin. Lipidol. 13, 373–381.
[21] Oram, J.F., Mendez, A.J., Slotte, J.P. and Johnson, T.F. (1991) Arterioscler Thromb 11, 403–414.
[22] Cavenagh, M.M., Whitney, J.A., Carroll, K., Zhang, C., Boman, A.L., Rosenwald, A.G., Mellman, I. and Kahn, R.A. (1996) J. Biol. Chem. 271, 21767–21774.
[23] D'Souza-Schorey, C., van Donselaar, E., Hsu, V.W., Yang, C., Stahl, P.D. and Peters, P.J. (1998) J. Cell Biol. 140, 603–616.
[24] Radhakrishna, H. and Donaldson, J.G. (1997) J. Cell Biol. 139, 49–61.
[25] Neufeld, E.B. et al. (2001) J. Biol. Chem. 276, 27584–27590.
[26] Neufeld, E.B., Demosky Jr., S.J., Stonik, J.A., Combs, C., Remaley, A.T., Duverger, N., Santamarina-Fojo, S. and Brewer Jr., H.B. (2002) Biochem. Biophys. Res. Commun. 297, 974–979.
[27] Takahashi, Y. and Smith, J.D. (1999) Proc. Natl. Acad. Sci. USA 96, 11358–11363.
[28] Schmitz, G., Robenek, H., Lohmann, U. and Assmann, G. (1985) EMBO J. 4, 613–622.
[29] Schmitz, G., Assmann, G., Robenek, H. and Brennhausen, B. (1985) Proc. Natl. Acad. Sci. USA 82, 6305–6309.
[30] Lin, C.Y. et al. (2000) J. Biol. Chem. 275, 37815–37823.
[31] Setty, S.R., Shin, M.E., Yoshino, A., Marks, M.S. and Burd, C.G. (2003) Curr. Biol. 13, 401–404.